Resonance Raman Spectra of $[M_6X_8Y_6]^{2-}$ Cluster Complexes (M = Mo, W; X, Y = Cl, Br, I)

Jon R. Schoonover,* Thomas C. Zietlow,† David L. Clark, Joseph A. Heppert,‡ Malcolm H. Chisholm,§ Harry B. Gray,† Alfred P. Sattelberger, and William H. Woodruff

Chemical Science and Technology Division, Los Alamos National Laboratory, Los Alamos, New Mexico 87545

Received February 22, 1996[⊗]

Resonance Raman spectra of the cubic metal−halide complexes having the general formula $[M_6X_8Y_6]^{2-}$ (M = Mo or W; X, Y = Cl, Br, or I) are reported. The three totally symmetric fundamental vibrations of these complexes are identified. The extensive mixing of the symmetry coordinates that compose the symmetric normal modes expected in these systems is not observed. Instead the "group-frequency" approximation is valid. Furthermore, the force constants of both the apical and face-bridging metal−halide bonds are insensitive to the identity of either the metal or the halide. Raman spectra of related complexes with methoxy and benzenethiol groups as ligands are reported along with the structural data for $[Mo_6Cl_8(SPh)_6][NBu_4]_2$. Crystal data for $[Mo_6Cl_8(SPh)_6][NBu_4]_2$ at −156 °C: monoclinic space group $P2_1/c$; a = 12.588(3), b = 17.471(5), c = 20.646(2) Å; β = 118.53(1)°, V = 3223.4 Å^3; d_{calcd} = 1.664 g cm^{-3}; Z = 2.

The chemistry, spectroscopy, and photophysics of metal−metal-bonded systems have been subjects of significant interest for over 2 decades.[1] These systems possess rich synthetic and structural chemistry, displaying chemical behavior and structural features of significance in many areas of chemistry, physics, and materials science. As this chemistry has evolved, however, spectroscopic and photophysical studies have generally been confined to binuclear complexes. Numerous metal clusters of higher nuclearity have now been characterized, and information on the spectroscopic properties of these complexes and the relationships of these properties to structure and dynamics is an important element of research associated with these clusters.

The molybdenum(II) and tungsten(II) halide clusters containing the $[M_6X_8]^{4+}$ core comprise an important, and in some senses archetypal, class of higher nuclearity transition metal cluster complexes. Their high symmetry, photochemical and photophysical properties, and structural relationships to cluster complexes of other elements are points of significant interest.[2−4] Furthermore, there is a structural similarity to ternary molybdenum chalcogenides known as Chevrel phases. The interesting properties (superconductivity, ordered magnetic phases, use as a solid electrolyte, hydrodesulfurization catalysis) of Chevrel phases are related to their structure, which consists of Mo_6Z_8 (Z = S, Se, or Te) clusters interlinked to form three-dimensional networks.[4,6]

The molybdenum− and tungsten−halide clusters exhibit exceptionally long-lived excited electronic states and undergo facile ground- and excited-state electron transfer.[2,7] This behavior is promising with regard to the potential incorporation of these systems into photochemical energy conversion schemes; in particular, the hexanuclear metal core and the long excited-state lifetimes may combine to permit multielectron excited-state redox reactivity. Toward this application, the photochemical properties of clusters with the $Mo_6Cl_8^{4+}$ core bound to silica gel have recently been investigated.[8] Clearly, the relationships among spectroscopy, structure, and photochemistry of these clusters merit investigation.

In this paper, we report a resonance Raman study of cluster complexes having the general formula $[M_6X_8Y_6]^{2-}$ [M = Mo(II), W(II)]. These complexes include binary and ternary metal−halide compounds (X, Y = Cl, Br, or I), complexes where X is the halide and Y is alkoxide or thiolate, as well as a compound where the X and Y ligands are both alkoxide. The structures of the halide complexes are known.[9−11] These clusters have full O_h symmetry with a $[M_6X_8]^{4+}$ core consisting of a regular octahedron of metal atoms inside, with face-bridging halide ions located at the vertices of the cube (Figure 1). The strong bonding in these clusters is exemplified by 2.62 Å Mo−Mo and 2.48 Å Mo−Cl distances in the octachlorohexamolybdate(II) ion.[11] The remaining six halides in the $[M_6X_8Y_6]^{2-}$ anion occupy apical positions on each vertex of the M_6 octahedron. The apical Mo−Cl distance is 2.50 Å in $(TBA)_2[M_6Cl_8Cl_6]$.[11] The apical halides tend to be substitutionally labile and are readily replaced by coordinating solvents.

† California Institute of Technology.
‡ University of Kansas.
§ Indiana University.
⊗ Abstract published in *Advance ACS Abstracts,* October 1, 1996.

(1) Cotton, F. A.; Walton, R. A. *Multiple Bonds Between Metal Atoms*; Oxford University Press: New York, 1993.
(2) Maverick, A. W.; Najdzionek, J. S.; MacKenzie, D.; Nocera, D. G.; Gray, H. B. *J. Am. Chem. Soc.* **1983**, *105*, 1878.
(3) Hughbanks, T.; Hoffmann, R. *J. Am. Chem. Soc.* **1983**, *105*, 1150.
(4) (a) Peña, O.; Sergent, M. *Prog. Solid State Chem.* **1989**, *19*, 165. (b) Yvon, K. In *Current Topics of Materials Science*, 1st ed.; Kaldis, E., Ed.; North Holland: New York, 1978; Vol. 3, Chapter 2.
(5) (a) Hilsenbeck, S. J.; McCarley, R. E. *Chem. Mater.* **1995**, *7*, 499. (b) Zhang, X.; McCarley, R. E. *Inorg. Chem.* **1995**, *34*, 2678. (c) Michel, J. B.; McCarley, R. E. *Inorg. Chem.* **1982**, *21*, 1864.
(6) (a) Mulhern, P. J.; Haering, R. R. *Can. J. Phys.* **1984**, *62*, 527. (b) McCarty, K. F.; Schrader, G. L. *Ind. Eng. Chem. Prod. Res. Dev.* **1984**, *23*, 519. (c) McCarty, K. F.; Andereff, J. W.; Schrader, G. L. *J. Catal.* **1985**, *93*, 375.
(7) (a) Maverick, A. W.; Gray, H. B. *J. Am. Chem. Soc.* **1981**, *103*, 1298. (b) Zietlow, T. C.; Nocera, D. G.; Gray, H. B. *Inorg. Chem.* **1986**, *25*, 1351.
(8) Robinson, L. M.; Lu, H.; Hupp, J. T.; Shriver, D. F. *Chem. Mater.* **1995**, *7*, 43.
(9) (a) Brosset, C. *Arkiv. Kemi. Mineral. Geol.* **1945**, *20A*, 7. (b) Brosset, C. *Arkiv. Kemi. Mineral. Geol.* **1946**, *22A*, 11.
(10) Vaughan, P. A. *Proc. Natl. Acad. Sci. U.S.A.* **1950**, *36*, 461.
(11) (a) Schafer, H.; Schnering, H. G.; Tillack, J.; Kuhnen, F.; Wohrle, H.; Baumann, H. *Z. Anorg. Chem.* **1967**, *353*, 218. (b) Schnering, H. G. *Z. Anorg. Chem.* **1971**, *385*, 75.

S0020-1669(96)00184-X CCC: $12.00

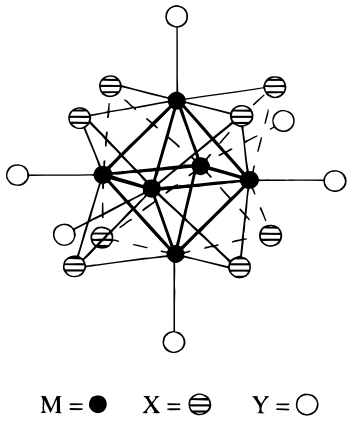

Figure 1. Structure of $[M_6X_8Y_6]^{2-}$, where M = Mo or W, X = Cl, Br, I, or OMe, and Y = Cl, Br, I, OMe, or SPh.

Several vibrational studies of the $[M_6X_8Y_6]^{2-}$ clusters have been published.[12−16] However, in some Raman spectra the number and symmetry of the observed Raman bands have been generally fewer than required by group theory. For example, two (rather than the predicted three) totally symmetric (A_{1g}) Raman bands have been identified. Given the extensive mixing of vibrations of the same symmetry that is anticipated in these systems, vibrational assignments remain ambiguous. A consequence is that accurate potential energy distributions cannot be calculated. Our objectives are to establish, if possible, complete ground-state Raman studies of these systems, arrive at reasonable vibrational assignments, and establish relationships between the Raman observables and the chemical and structural features in these clusters.

Experimental Section

Physical Measurements. Raman spectra were measured by using a SPEX 1403 or a SPEX Ramanlog EU spectrometer equipped with an RCA 3034A photomultiplier tube, an ORTEC 9300 series photon counter, and a Nicolet 1180E Raman data system. The various laser excitation lines were supplied by a Spectra-Physics 171-01 Kr^+, 171-19 Ar^+, or 164 Ar^+ laser. The spectra were measured at a scan rate of 1 cm^{-1} s^{-1}, a spectral slit width of 4 cm^{-1}, and a laser power between 5 and 50 mW incident on the sample. The sampling arrangement consisted of a 135° backscattering geometry with solutions contained in an NMR tube or powdered samples in a capillary. Powdered samples were diluted with KCl or KBr. Infrared spectra were recorded either on a Bio-Rad FTS 40 spectrophotometer as petroleum jelly mulls between polyethylene plates or on a Perkin-Elmer 283 as Nujol mulls between CsI plates. ^1H NMR spectra of the thiolate derivative were recorded on a Nicolet NT-360 spectrometer at 360 MHz in dry, oxygen-free acetonitrile-d_3. ^1H NMR chemical shifts are reported in ppm relative to the CHD_2 quintet of acetonitrile-d_3 set at δ 1.93.

Synthesis and General Procedures. All reactions were carried out under an atmosphere of dry, oxygen-free nitrogen using standard Schlenk and glovebox techniques. Solvents for syntheses were degassed, distilled, and stored under nitrogen and over sieves. Molybdenum metal and $MoCl_5$ were purchased from Pressure Chemical and used without further purification. Sodium metal was purchased from Aldrich and used without further purification.

Most spectroscopic studies employed tetrabutylammonium (TBA) salts of cluster anions, except for $Na_2[Mo_6Cl_8(OMe)_6]$. $Mo_6Cl_8Cl_4$ and $Na_2[Mo_6Cl_8Cl_6]$ were prepared by the method of Nanelli and Block.[17] The sodium salt was converted to TBA salt by simple metathesis with (TBA)Cl in CH_3CN. The corresponding bromide and iodide complexes were prepared by alkali melt reactions as described by Sheldon.[18] The Raman spectra of the iodide clusters demonstrated the presence of triiodide impurity. The $(TBA)_2[W_6Cl_8Cl_6]$ cluster was prepared by the method of Hogue and McCarley,[14] while the other tungsten−halide clusters were prepared by the alkali melt reaction described by Sheldon.[18] The mixed-halide cluster, $(TBA)_2[W_6Br_8Cl_6]$, was prepared by reflux and repeated recrystallization of the hydronium salt of $[W_6Br_8Br_6]^{2-}$ in aqueous HCl solution, followed by treatment of the aqueous HCl solution with (TBA)Cl. The methoxy clusters, $[Mo_6Cl_8(OMe)_6]^{2-}$ and $[Mo_6(OMe)_8(OMe)_6]^{2-}$, were prepared by the method of Nannelli and Block.[19] The thiolate derivative, $[Mo_6Cl_8(SPh)_6]^{2-}$, can be prepared by several routes, the most fruitful of which are outlined in the following.

Synthesis of $(TBA)_2[Mo_6Cl_8(SPh)_6]$. Procedure I. In a Schlenk reaction vessel, $Na_2[Mo_6Cl_8(OMe)_6]$ (0.60 g, 0.55 mmol) was taken up as a slurry in 5 mL of THF and 10 equiv (5.5 mmol) of thiophenol was added. Within several minutes after the addition of thiophenol, all of the solids had dissolved and the solution turned dark orange-brown. The solution was heated to reflux and allowed to cool slowly to room temperature. After cooling, (TBA)Br (1.10 mmol) was added and the solution stirred for several hours. Reaction solvents were removed in vacuo and the solids extracted with CH_3CN (10 mL). The volume of solution was reduced to ca. 1 mL and cooled to −20 °C. After several days, large orange-brown crystals were isolated by cannula filtration and dried in vacuo. Total yield = 0.61 g.

Procedure II. In a Schlenk reaction vessel, NaSPh (28 mmol) was prepared by warming Na metal (0.65 g, 28 mmol) and PhSH (28 mmol) in 20 mL of THF. After dissolution of the Na, the THF solvent was removed in vacuo and the solid NaSPh dissolved in MeOH (50 mL). To a stirring solution was added Mo_6Cl_{12} (2.0 g, 2 mmol) from a solids addition tube, and the stirring solution was refluxed for 2 h. Upon cooling, a white precipitate was removed by filtration. The reflux condenser was replaced by a short-path distillation head, and the MeOH was distilled from the deep orange solution to near dryness (110 °C), resulting in a bright orange residue. The residue was cooled to room temperature then taken up in MeOH, and the volume was reduced until orange crystals formed. The crystals were redissolved by warming the solution to 60 °C, after which it was allowed to cool slowly to room temperature, producing small orange crystals. The solution was cooled to −15 °C for 24 h, which produced numerous orange crystals and some yellow precipitate. The crystals were isolated by cannula filtration. A second crop of crystals was obtained by reducing the volume of filtrate and cooling. Total yield = 2.07 g of $Na_2[Mo_6Cl_8(SPh)_6]$. The latter salt was dissolved in 5 mL of MeOH and 2 mL of CH_3CN, and (TBA)Br (0.65 g) was added. The solution was allowed to stand for several hours, resulting in the precipitation of the white solid, which was removed by filtration. Anal. Calcd for $Mo_6Cl_8S_6C_{68}H_{102}N_2$: C, 40.85; H 5.14; N, 1,40; S, 9.62; Cl, 14.19. Found: C, 41.84; H, 5.22; N, 1.42; S, 9.52; Cl, 14.01. ^1H NMR at 360 MHz, 22 °C in CD_3CN: $\delta[(N_9C_4H_9)_4]$ 1.0 (t, 24H), 1.4 (mult, 16H), 1.6 (mult, 16H), 3.1 (mult, 16H); $\delta(SC_6H_5)$ 7.15 (mult, 30H).

Crystal Structure Analysis of $(TBA)_2[Mo_6Cl_8(SPh)_6]$. General operating procedures and listings of programs have been previously reported.[20] A suitable fragment was cleaved from a larger clump of crystals by using standard inert atmosphere handling techniques. The sample was transferred to the goniostat of the diffractometer, cooled to −160 °C, and characterized by using a reciprocal lattice search technique. The structure was solved by direct methods (MULTAN 78) and Fourier techniques and refined by full-matrix least squares.

(12) Clark, R. J. H.; Kepert, D. L.; Nyholm, R. S.; Rodley, G. A. *Spectrochim. Acta* **1966**, *22*, 1697.
(13) Cotton, F. A.; Wing, R. M.; Zimmerman, R. H. *Inorg. Chem.* **1967**, *6*, 11.
(14) Hogue, R. D.; McCarley, R. E. *Inorg. Chem.* **1970**, *9*, 1354.
(15) Hartley, D.; Ware, M. J. *Chem. Commun.* **1967**, 912.
(16) (a) Mancour, S.; Caillet, P.; Jouan, M.; Dao, N. Q. *J. Raman Spect.* **1987**, *18*, 177. (b) Zelverte, A.; Mancour, S.; Caillet, P. *Spectrochim. Acta* **1986**, *42A*, 837. (c) Mancour, S.; Caillet, J. *J. Phys. Chem. Solids* **1988**, *49*, 1071. (d) Mancour, S.; Potel, M.; Caillet, J. *J. Mol. Struct.* **1987**, *162*, 1.
(17) Nannelli, P.; Block, B. P. *Inorg. Synth.* **1970**, *12*, 170.
(18) (a) Sheldon, J. C. *J. Chem. Soc.* **1960**, 1007, 3106. (b) Sheldon, J. C. *J. Chem. Soc.* **1962**, 410. (c) Sheldon, J. C. *J. Chem. Soc.* **1963**, 4183. (d) Sheldon, J. C. *J. Chem. Soc.* **1964**, 1287.
(19) (a) Nannelli, P.; Block, B. P. *Inorg. Chem.* **1968**, *7*, 2423. (b) Nannelli, P.; Block, B. P. *Inorg. Synth.* **1972**, *13*, 99.
(20) Chisholm, M. H.; Folting, K.; Huffman, J. C.; Kirkpatrick, C. C. *Inorg. Chem.* **1984**, *23*, 1021.

Table 1. Crystallographic Data for $[Mo_6Cl_8(SPh)_6][NBu_4]_2$

empirical formula	$[C_{66}H_{30}S_6Cl_8Mo_6][NC_{16}H_{36}]_2$
color, habit	yellow
crystal dimen, mm^{-1}	$0.18 \times 0.18 \times 0.22$
space group	$P2_1/c$
cell dimens	
a, Å	12.588(3)
b, Å	17.471(5)
c, Å	20.646(6)
β, deg	118.53(1)
volume, Å^3	3989.08
Z, molecules/cell	2
formula weight	1999.19
D_{calc}, g cm^{-3}	1.664
absorption coefficient, cm^{-1}	13.541
λ (Mo Kα)	0.71069
temperature, °C	−156
2θ range, deg	6.0−45.0
measured reflections	7286
unique intensities	5243
observed reflections	4837 ($F > 2.33\sigma(F)$)
$R(F)$[a]	0.0252
$R_w(F)$[b]	0.0314
goodness-of-fit	0.823

[a] $R = \sum||F_o| - |F_c||/\sum|F_o|$. [b] $R_w = [(\sum w(|F_o| - |F_c|)^2/\sum w(F_o)^2]^{1/2}$.

All hydrogen atoms were clearly visible in a difference Fourier phased on the non-hydrogen atoms and were refined isotropically. A final difference Fourier was featureless, the largest peak being 0.32 e/Å^3.

Pertinent distances and angles (averaged) for the $[Mo_6Cl_8(SPh)_6]^{2-}$ anions are Mo−Mo = 2.623(1) Å, Mo−Cl = 2.479(3) Å, Mo−S = 2.489(3) Å, Mo−S−C = 111.1(3)°, and Mo−Cl−Mo = 63.9(1)° (Table 1). Full crystal structure data are presented in the supporting information.

Results and Discussion

Symmetry Considerations. The selection rules for $M_6X_8Y_6$ complexes, which belong to the point group O_h, are summarized in Table 2. Ten modes are Raman active ($3A_{1g} + 3E_g + 4T_{2g}$) with five infrared active modes ($5T_{1u}$). It is important to note, however, that the symmetry may be degraded by the environment of the molecules in crystalline compounds, and if this occurs, more (but never fewer) than the predicted number of vibrations may be observed. The symmetry coordinates of the three totally symmetric Raman active fundamentals consist of the breathing motions of the M_6 cage, X_8 face-bridging cube, and the apical Y_6 structures. The normal modes composed of these symmetry coordinates may be identified by their total polarization in the Raman spectra ($\rho = I_\perp/I_{||} = 0$). The structure of these complexes is such that the symmetry coordinates are expected to be extensively mixed in forming the normal modes. For example, the metal−metal cage breathing coordinate might be expected to mix extensively with the face-bridging metal−halide breathing coordinates since displacement of the metal−metal bonds cannot occur without simultaneously affecting the metal−halide bonds. Accordingly, the three symmetric normal modes would comprise a weighted mixture of the three symmetry coordinates. Some have suggested, quite reasonably given the foregoing arguments, that the "group-frequency" concept is invalid when analyzing the $[M_6X_8Y_6]^{2-}$ clusters.[15] The Raman data in this study demonstrate that, contrary to expectations, these complexes behave very much as if the symmetric normal modes are accurately represented by the unmixed symmetry coordinates. Experimentally, the breathing modes of the M_6 cage, the X_8 cube, and the apical Y_6 cage act as group frequencies.

Clusters with $Mo_6Cl_8^{4+}$. The Raman shifts in wavenumber and proposed assignments for the Raman spectra of complexes with an octachlorohexamolybdate(II) unit and $(TBA)_2[Mo_6(OMe)_8(OMe)_6]$ are listed in Table 3. The spectra of a powdered sample of $(TBA)_2[Mo_6Cl_8Cl_6]$ and $Mo_6Cl_8Cl_4$ in THF are compared in Figure 2, and the spectra of $Na_2[Mo_6Cl_8(OMe)_6]$ and $(TBA)[Mo_6(OMe)_8(OMe)_6]$ are shown in Figure 3. The number of fundamentals observed in the Raman spectrum of $(TBA)_2[Mo_6Cl_8Cl_6]$ agrees with the predictions from group theory. Two of the three symmetric modes for this complex are readily identified when all of the data in Table 3 are considered. The polarized band at 236 cm^{-1} is assigned to the apical Y_6 breathing mode. This band shifts as Y is changed,

Table 2. Selection Rules for $M_6X_8Y_6$ Species in the Point Group O_h[a]

internal coordinates	symmetry elements									
	A_{1g}	A_{2g}	E_g	T_{1g}	T_{2g}	A_{1u}	A_{2u}	E_u	T_{1u}	T_{2u}
M−M(12)	1		1		1				1	1
M−X(24)	1		1	1	2		1	1	2	1
M−Y(6)	1		1						1	
X−M−Y(12)				1	1				1	1

[a] Raman active: $3A_{1g} + 3E_g + 4T_{2g}$. Infrared active: $5T_{1u}$.

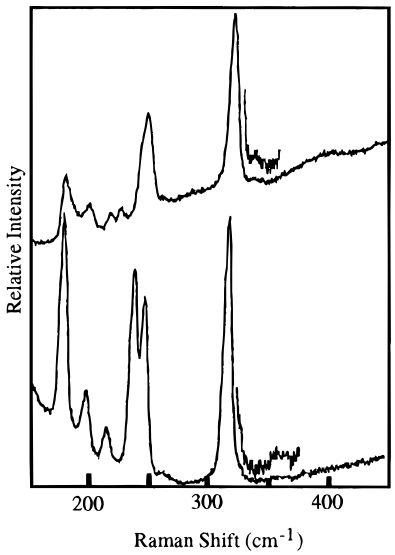

Figure 2. Comparison of the resonance Raman spectra of $[Mo_6Cl_8(Cl_4(THF)_2)]$ in THF (top) and $(TBA)_2[Mo_6Cl_8Cl_6]$ as a solid diluted with KCl (bottom). Laser excitation was 488.0 nm for $[Mo_6Cl_8(Cl_4(THF)_2)]$ and 482.5 nm for $(TBA)_2[Mo_6Cl_8Cl_6]$.

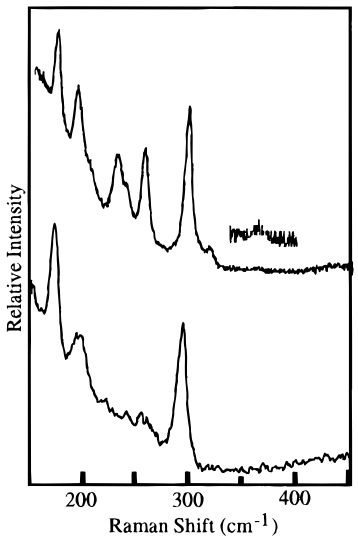

Figure 3. Comparison of the resonance Raman spectra of $Na_2[Mo_6Cl_8(OMe)_6]$ (top) and $(TBA)_2[Mo_6(OMe)_8(OMe)_6]$ (bottom) as solids. Laser excitation was 514.5 nm for $Na_2[Mo_6Cl_8(OMe)_6]$ and 647.1 nm for $(TBA)_2[Mo_6(OMe)_8(OMe)_6]$.

Table 3. Raman Shifts (cm^{-1}) and Proposed Assignments for Mo Clusters[a]

	$Mo_6Cl_8Cl_4$					
$(TBA)_2[Mo_6Cl_8Cl_6]$	in THF	solid	$Na_2[Mo_6Cl_8(OMe)_6]$	$(TBA)_2[Mo_6Cl_8(SPh)_6]$	$(TBA)[Mo_6(OMe)_8(OMe)_6]$	assignments
47				68		
96		110		82		X−Mo−Y, T_{2g}
124		117		146	133	
176	176	179	172	175	171	Mo−Mo
	183			153		
196	197	191	191	192	196	Mo−Mo
	202	197				Mo−O
213	215	218	204	208		Mo−Cl
236p	224p	248	229	169p	222	Mo−Y(Y_6), A_{1g}
	240p				241	Mo−O(Y)
245	246		238	241		Mo−Cl
264	260	265	255	220	257	Mo−Y, E_g
	277		303	252	292	
314p	316p	319	295p	312p		Mo−Cl(X_8), A_{1g}
320	320		316	324		Mo−Cl
				287p		SPh mode
355	336p	368	358	338	366	Mo−Mo(M_6), A_{1g}
				351		
				422		SPh mode
				431		SPh mode

[a] p signifies polarized vibration where depolarization ratios were measured.

both in the complexes listed in Table 3 and in the previously reported spectra of a $[Mo_6Cl_8Y_6]^{2-}$ series.[15] The breathing motion of the face-bridging Cl_8 cube is identified as the intense, polarized band at 314 cm^{-1}; it is present in this region in all compounds containing the $Mo_6Cl_8^{4+}$ unit.

To confirm these assignments and identify the third symmetric fundamental, the spectra of the $(TBA)_2[Mo_6X_8Y_6]$ (X, Y = Cl, Br, or I) complexes are considered (Table 4). The bands assigned to the Y_6 and X_8 breathing modes show the expected shifts when the halides are changed from Cl to Br to I. The third symmetric mode is identified as bands in the spectra of $(TBA)_2[Mo_6Br_8Br_6]$ at 326 cm^{-1} and $(TBA)_2[Mo_6I_8I_6]$ at 292 cm^{-1}. These bands can be assigned to the Mo_6 cage breathing motion. The symmetric Mo_6 vibration is then assigned in $(TBA)_2[Mo_6Cl_8Cl_6]$ to one of the weak features at either 320 or 355 cm^{-1}. The depolarization ratio of these two bands could not be measured due to their low intensity and, in the case of the 320 cm^{-1} band, proximity to the intense 314 cm^{-1} Raman band. The weak intensity of the band assigned to the Mo_6 A_{1g} vibration in $(TBA)_2[Mo_6Cl_8Cl_6]$ may be rationalized by suggesting that the internal symmetry coordinate represented by the Mo_6 cage mode contributes to normal modes wherein the Mo_6 unit vibrates in phase and out of phase with the Y_6 breathing motion. The in-phase normal mode (predominantly the Y_6 breathing motion) results in a large change in polarizability and thus an intense Raman band. The out-of-phase normal mode (predominantly the Mo_6 breathing motion) involving these two symmetry coordinates results in a small overall change in polarizability, resulting in a weak Raman band. This effect is most pronounced when the natural, unmixed frequencies of the symmetry coordinates are close to the same, as is the case with Y = Cl. However, when the halides are changed from chloride to bromide or iodide, the in-phase/out-of-phase character of the resulting normal modes is less pronounced because of energy factoring of the contributing symmetry coordinates.

It is informative at this point to compare the Raman spectrum of $Mo_6Cl_8Cl_4$ to that of $(TBA)_2[Mo_6Cl_8Cl_6]$ and their corresponding assignments. For $Mo_6Cl_8Cl_4$ as a solid, the four apical chlorides act as bridges between adjacent $Mo_6Cl_8^{4+}$ units.[21] In THF, as in various other solvents, the complex takes the form $[Mo_6Cl_8(Cl_4(THF)_2)]$.[12,21] The spectrum of this complex is then quite similar to that of $(TBA)_2[Mo_6Cl_8Cl_6]$ as illustrated in Figure 2. This observation demonstrates that the change in Y ligands from Cl to an oxygen donor does not grossly affect the symmetry of the molecule. Bands for four totally symmetric vibrations in $[Mo_6Cl_8(Cl_4(THF)_2)]$ are identified; the Cl_6 (240 cm^{-1}), Cl_8 (316 cm^{-1}), and Mo_6 (336 cm^{-1}) breathing modes are assigned on the basis of depolarization ratio measurements and the arguments proposed earlier. The new polarized band at 224 cm^{-1} may then be associated with a Mo−O(THF) vibration. ν(M−O) bands have been identified near 230 and 250 cm^{-1} in $[Mo_6O_x]$ (x = 17, 18, or 19) and $(TBA)_2[Mo_6Cl_8(CF_3COO)_6]$ complexes.[22a,b] The weak feature located at 260 cm^{-1} in the $[Mo_6Cl_8(Cl_4(THF)_2)]$ spectrum and at 264 cm^{-1} in the $(TBA)_2[Mo_6Cl_8Cl_6]$ spectrum is not present in any of the remaining complexes in Table 3 and may then be attributed to the Mo−Y(Cl) E_g vibration.

Comparison of the Raman spectra of $(Na)_2[Mo_6Cl_8(OMe)_6]$ and $(TBA)_2[Mo_6Cl_8(SPh)_6]$ to the aforementioned results assists in the assignment of bands due to the $Mo_6Cl_8^{4+}$ unit. Additional comparison to the $(TBA)_2[Mo_6(OMe)_8(OMe)_6]$ spectrum allows the assignment of bands exclusively due to the metal octahedron. The spectra of the two methoxy clusters are shown in Figure 3. The Raman spectrum of $(Na)_2[Mo_6Cl_8(OMe)_6]$ exhibits Raman shifts not observed in the spectrum of $(TBA)_2[Mo_6Cl_8Cl_6]$. Fundamentals at 229 and 255 cm^{-1} can be attributed to Mo−O vibrations associated with the apical methoxy ligands. Depolarization ratios could not be measured due to substitutional lability in solution. The polarized band at 295 cm^{-1} can be assigned to the Cl_8 A_{1g} mode, while the symmetric Mo_6 motion may be attributed to a weak feature at either 318 or 358 cm^{-1}.

The Raman spectrum of the thiolate derivative exhibits strong bands at 169, 241, 287, 312, and 422 cm^{-1}. The polarized band at 169 cm^{-1} is assigned to the symmetric Y_6 breathing mode, while the polarized band at 312 cm^{-1} is attributed to the Cl_8 breathing mode. The band at 287 cm^{-1} is also polarized and could be assigned to the Mo_6 A_{1g} vibration,

(21) Schafer, H.; Schnering, H. G. *Angew. Chem.* **1964**, *76*, 833.

(22) (a) Proust, T.; Thouvenot, R.; Chaussade, M.; Robert, F.; Gouzerh, P. *Inorg. Chim. Acta* **1994**, *224*, 81. (b) Harder, K.; Preetz, W. *Z. Anorg. Allg. Chem.* **1992**, *612*, 97. (c) Adams, R. W.; Martin, R. L.; Winter, G. *Aust. J. Chem.* **1967**, *20*, 773. (d) Mehrotra, R. C.; Batwara, J. M. *Inorg. Chem.* **1970**, *9*, 2505. (e) Barroclough, C. G.; Badley, D. C.; Lewis, J.; Thomas, I. M. *J. Chem. Soc.* **1961**, 2601.

but the Mo−Mo bond distance suggests a value closer to that observed in other Mo_6 clusters (*vide infra*). We therefore assign this mode to the weak band at 338 cm^{-1}. The intense bands at 287 and 422 cm^{-1} are not observed in any other clusters, which suggests that they originate from vibrations associated with internal ligand modes of benzenethiol.

Bands due to asymmetric vibrations that are present in the spectra of the series with the $Mo_6Cl_8^{4+}$ unit, including $(Na)_2[Mo_6Cl_8(OMe)_6]$ and $(TBA)_2[Mo_6Cl_8(SPh)_6]$, but that are not observed in the $(TBA)_2[Mo_6(OMe)_8(OMe)_6]$ spectrum can be assigned to face-bridging Mo−Cl vibrations. These features include the strong Raman band near 245 cm^{-1} and the medium-strong band near 210 cm^{-1} (Table 3). In addition to a band assigned to the A_{1g} metal cage breathing mode, two other Raman bands (near 175 and 195 cm^{-1}) are observed in all complexes listed in Table 3. These two fundamentals can be assigned to the two remaining Mo−Mo modes (E_g and T_{2g}). This leaves the other bands (222, 241, 257, and 292 cm^{-1}) in the spectrum of $(TBA)_2[Mo_6(OMe)_8(OMe)_6]$ to be attributed to Mo−O vibrations. The bands at 222 and 257 cm^{-1} compare well to the bands at 229 and 255 cm^{-1} observed in the $(Na)_2[Mo_6Cl_8(OMe)_6]$ spectrum and can be ascribed to Mo−Y(O) vibrations. The band at 241 cm^{-1} is then assigned to a Mo−X(O) vibration. The Raman shifts for the Mo−O vibrations agree with data for Mo−O vibrations in related complexes.[22] Depolarization ratio measurements could not be made due to the the low intensity of these bands. These Mo−O vibrations are likely too low in frequency to be associated with A_{1g} modes of the $(OMe)_8$ or $(OMe)_6$ entities; a more plausible assignment is the bending motions associated with these ligands.[22c−e]

No Raman band attributable to the A_{1g} Mo_6 mode is observed in the spectrum of $(TBA)_2[Mo_6(OMe)_8(OMe)_6]$ in the same region as noted in the $(Na)_2[Mo_6Cl_8(OMe)_6]$ spectrum. This observation can be explained when the Mo−Mo distances of these two clusters are compared.[23] Little change in the Mo−Mo distance is observed upon substitution of OMe for Cl in the apical or Y position (2.607 vs 2.620 Å). However, replacement of face-bridging Cl by OMe results in a substantial shortening of the Mo−Mo bond length to 2.536 Å. This shorter bond distance is reflected in the Raman spectrum by a shift of the band attributed to the A_{1g} Mo_6 mode to higher energy (366 cm^{-1}).

The assignments of the symmetric Mo_6 cage breathing mode can be further examined by comparing the experimental results to data calculated from an empirical relationship between bond distances and force constants.[24] The comparison of observed and calculated Raman shifts is presented in Table 4. Crystal structure data reveal that the differences in Mo−Mo distances parallel the observed variations in the Raman shift.[19,23,25,26] The calculated data further indicate that when there is an inconclusive band assignment for the A_{1g} Mo_6 mode, the higher frequency band is the more reasonable assignment. Therefore, the symmetric Mo_6 mode is assigned to the 358 cm^{-1} band for $(Na)_2[Mo_6Cl_8(OMe)_6]$, the 355 cm^{-1} band for $(TBA)_2[Mo_6Cl_8Cl_6]$, and the 338 cm^{-1} band for $(TBA)_2[Mo_6Cl_8(SPh)_6]$. The variations in the observed shift of the A_{1g} Mo_6 band are almost entirely accounted for by differences in the Mo−Mo force constant that accompany the dissimilarities in the Mo−Mo bond distances and not by differences in mixing of the Mo−Mo and Mo−X or Mo−Y coordinates.

Table 4. Raman Shifts and Proposed Assignments for $(TBA)_2[Mo_6X_8Y_6]$ Series (X = Y = Cl, Br, or I)[a]

$(TBA)_2$-$[Mo_6Cl_8Cl_6]$	$(TBA)_2$-$[Mo_6Br_8Br_6]$	$(TBA)_2$-$[Mo_6I_8I_6]$	assignment
47			
96	62	46	X−Mo−Y, T_{2g}
124	67	60	
176	120	92	Mo−Mo
196	126	108	Mo−Mo
213	136		Mo−X
236p	154p	113p	Mo−Y(Y_6), A_{1g}
245	170	130	Mo−X
264			Mo−Y, E_g
314p	205p	155p	Mo−X(X_8), A_{1g}
320	262	213	Mo−X
355	326p	292p	Mo−Mo(M_6), A_{1g}
		285	

[a] p signifies a polarized vibration where depolarization ratios were measured; excitation wavelengths as in figure captions.

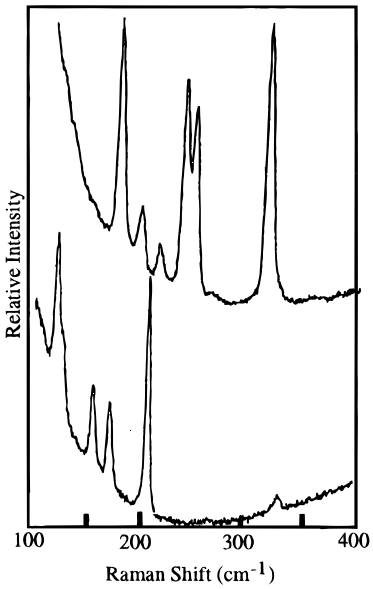

Figure 4. Resonance Raman spectra of $(TBA)_2[Mo_6Cl_8Cl_6]$ (top, 482.5 nm) and $(TBA)_2[Mo_6Br_8Br_6]$ (bottom, 514.5 nm). Samples were diluted with KCl and KBr, respectively; the spectra were measured on powders.

$[Mo_6X_8Y_6]^{2-}$ Clusters (X = Y). The Raman shifts and proposed assignments for the molybdenum−halide cluster series are given in Table 4, and the spectra of the chloro and bromo complexes are compared in Figure 4. The lowest frequency polarized band in all cases is identified as the A_{1g} Y_6 breathing mode. This assignment agrees with the data for the previously reported $[Mo_6Cl_8Y_6]^{2-}$ series.[15] This band decreases from 236 to 154 to 113 cm^{-1} when changing the halide from Cl to Br to I for the $(TBA)_2[Mo_6X_8Y_6]$ series (X = Y), while for the $[Mo_6Cl_8Y_6]^{2-}$ series it changes from 236 to 160 to 117 cm^{-1}, respectively.[15] The other intense, polarized band that decreases by approximately the same factor with changing halides is attributed to the A_{1g} X_8 breathing motion. It is observed at 314 cm^{-1} in the spectrum of $(TBA)_2[Mo_6Cl_8Cl_6]$, at 205 cm^{-1} for $(TBA)_2[Mo_6Br_8Br_6]$, and at 155 cm^{-1} for $(TBA)_2[Mo_6I_8I_6]$. The A_{1g} Mo_6 cage mode is a weak band in all of the molybdenum−halide cluster spectra, but can be identified by depolarization ratio measurements for $[Mo_6Br_8Br_6]^{2-}$ (326 cm^{-1}) and $[Mo_6I_8I_6]^{2-}$ (292 cm^{-1}). As discussed earlier, the band at 355 cm^{-1} is assigned to this mode for $(TBA)_2[Mo_6Cl_8Cl_6]$. Tentative assignments for the remaining Raman bands are listed

(23) Chisholm, M. H.; Heppert, J. A.; Huffman, J. C. *Polyhedron* **1984**, *3*, 475.
(24) Conradson, S. D.; Sattelberger, A. P.; Woodruff, W. H. *J. Am. Chem. Soc.* **1988**, *110*, 1309.
(25) Guggenberger, L. J.; Sleight, A. W. *Inorg. Chem.* **1969**, *8*, 2041.
(26) Zietlow, T. C.; Schaefer, W. P.; Sadeghi, B.; Hua, H.; Gray, H. B. *Inorg. Chem.* **1986**, *25*, 2195, 2198.

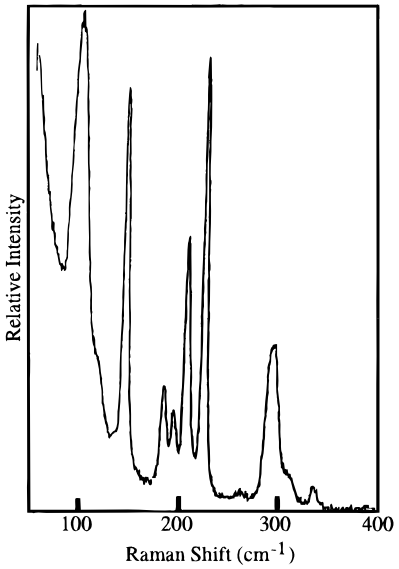

Figure 5. Resonance Raman spectrum of $(TBA)_2[W_6Cl_8Cl_6]$ measured with 482.5 nm laser excitation.

in Table 4. These assignments were made by using the data in Table 3 and intensity arguments.

Mancour et al. have suggested an alternative assignment for the Mo−Mo A_{1g} mode by using Raman data measured on single crystals of $Cd[Mo_6Cl_8Cl_6]$ and $Cd[Mo_6Br_8Br_6]$.[16] Intense Raman bands between 100 and 110 cm^{-1} demonstrate variations in intensity with laser light of different directions of polarization. These bands were assigned to the symmetric Mo_6 vibration. In contrast, the only Raman bands near this frequency in our solution spectra are at 96 cm^{-1} for $(TBA)_2[Mo_6Cl_8Cl_6]$ and 120 cm^{-1} for $(TBA)_2[Mo_6Br_8Br_6]$. Depolarization ratio measurements of these bands in solution show that they are asymmetric vibrations. The intense band at 96 cm^{-1} for $(TBA)_2[Mo_6Cl_8Cl_6]$ is more likely associated with intense bands at 61 cm^{-1} for $(TBA)_2[Mo_6Br_8Br_6]$ and at 46 cm^{-1} for $(TBA)_2[Mo_6I_8I_6]$. Hartley and Ware also observed intense bands for $[Mo_6Cl_8Cl_6]^{2-}$ (92 cm^{-1}), $[Mo_6Cl_8Br_6]^{2-}$ (60 cm^{-1}), and $[Mo_6Cl_8I_6]^{2-}$ (44 cm^{-1}) in methanol.[15] Similar bands are also found in this region for the analogous tungsten clusters: $(TBA)_2[W_6Cl_8Cl_6]$, 98 cm^{-1}; $(TBA)_2[W_6Br_8Cl_6]$, 93 cm^{-1}; $(TBA)_2[W_6Br_8Br_6]$, 62 cm^{-1}; $(TBA)_2[W_6I_8I_6]$, 44 cm^{-1}. The variation with changing Y ligand suggests the assignment of these bands to an M−Y stretch or the X−M−Y bend. In far-infrared spectra, the X−M−Y bend varies in a similar manner.[14] The Mo−Mo A_{1g} vibration is more reasonably associated with the 371 cm^{-1} band in the $Cd[Mo_6Cl_8Cl_6]$ spectrum from Mancour et al. Its intensity pattern is similar to those of other A_{1g} modes.[16]

$(TBA)_2[W_6X_8Y_6]$ Clusters. In the $(TBA)_2[W_6X_8Y_6]$ series, the Raman bands due to the Y_6 and X_8 symmetric breathing motions are identified by their depolarization ratios; as expected, they decrease in frequency according to Cl > Br > I. The Raman shifts of the band assigned to the A_{1g} Y_6 mode are 225, 161, and 131 cm^{-1}, and the bands attributed to the symmetric X_8 mode are 296, 198, and 152 cm^{-1} for the chloro, bromo, and iodo clusters, respectively. The Raman spectrum of $(TBA)_2[W_6Cl_8Cl_6]$ is shown in Figure 5, and the $(TBA)_2[W_6Br_8Br_6]$ and $(TBA)_2[W_6Br_8Cl_6]$ spectra are compared in Figure 6 with the Raman shifts and proposed assignments in Table 6. The assignments of the A_{1g} fundamentals are reinforced with data from $(TBA)_2[W_6Br_8Cl_6]$. The Raman spectrum of this cluster exhibits a band at 218 cm^{-1} due to the Cl_6 cage breathing mode; an analogous band is at 225 cm^{-1} in the spectrum of $(TBA)_2[W_6Cl_8Cl_6]$. The symmetric Br_8 mode is identified as the Raman band at 197 cm^{-1} in the spectrum of $(TBA)_2[W_6Br_8Cl_6]$ and that at 198 cm^{-1} for $(TBA)_2[W_6Br_8Br_6]$. The symmetric W_6 cage vibration in the spectrum of $(TBA)_2[W_6Cl_8Cl_6]$ can be assigned to the polarized band at 289 cm^{-1}, which overlaps the Cl_8 breathing mode. The band centered at 294 cm^{-1} is two overlapping bands (296 and 289 cm^{-1}) both of which are polarized vibrations. The band due to the A_{1g} W_6 mode is also identified by depolarization ratio measurements in the spectrum of the tungsten−bromide cluster at 271 cm^{-1} and in the spectrum of the tungsten−iodide cluster at 236 cm^{-1}. The weak 268 cm^{-1} feature in the spectrum of $(TBA)_2[W_6Br_8Cl_6]$ can be assigned to this mode. Assignments of bands due to asymmetric vibrations (Table 6) were made by comparison to the molybdenum complexes.

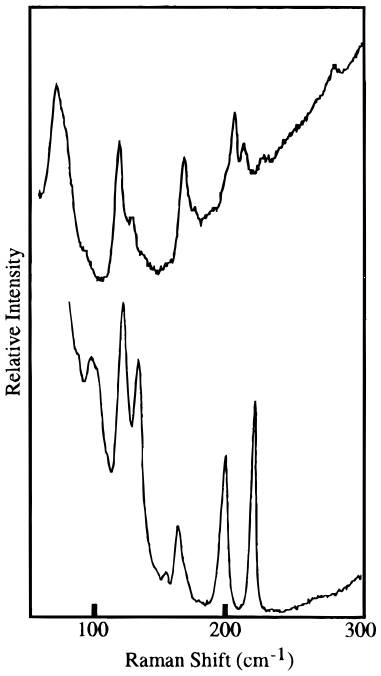

Figure 6. Comparison of the resonance Raman spectra of $(TBA)_2[W_6Br_8Br_6]$ (top) and $(TBA)_2[W_6Br_8Cl_6]$ (bottom) measured with 514.5 nm laser excitation.

Table 5. Calculated and Observed Raman Shifts for the Bands Assigned to the Symmetric Mo_6 Cage Breathing Mode[a]

complex	Raman shift (cm^{-1}) calculated	observed	Mo−Mo distance (Å) (ref)
$(TBA)[Mo_6(OMe)_8(OMe)_6]$	360	366	2.536 (23)
$Na_2[Mo_6Cl_8(OMe)_6]$	338	358	2.607 (23)
$(TBA)_2[Mo_6Cl_8Cl_6]$	332	355	2.620 (11)
$[Mo_6Cl_8(Cl_4(THF)_2)]$	332	336	2.62 (9)
$(TBA)_2[Mo_6Cl_8(SPh)_6]$	332	338	2.623 (this work)
$(TBA)_2[Mo_6Br_8Br_6]$	326	326	2.64 (25)

[a] Equations are from ref 24 and calculations were made with $(TBA)_2[Mo_6Br_8Br_6]$ as the reference.

Comparison of $(TBA)_2[W_6Br_8Br_6]$ and $(PPN)[W_6Br_8Br_6]$. The oxidation of $(TBA)_2[W_6Br_8Br_6]$ adds positive charge to the W_6 octahedron, causing a lengthening of the metal−metal bonds while the metal−bromide bonds shorten. This fact is established by the crystal structures of $(TBA)_2[W_6Br_8Br_6]$ and $(PPN)[W_6Br_8Br_6]$ (PPN is $((C_6H_5)_3P_2N^+)$].[26] By using these bond distances, a force constant relationship, and polarization data, the energies of the three symmetric modes may be compared (Table 7). The Raman bands due to the A_{1g} Br_6 and Br_8 modes in $(PPN)[W_6Br_8Br_6]$ are assigned by their polarization and match well with the calculated data. The apical W−Br bond distance shortens in the reduced form with a corresponding shift for the

Table 6. Raman Shifts (cm^{-1}) and Proposed Assignments for $(TBA)_2[W_6X_8Y_6]$ Series[a]

$(TBA)_2$-$[W_6Cl_8Cl_6]$	$(TBA)_2$-$[W_6Br_8Cl_6]$	$(TBA)_2$-$[W_6Br_8Br_6]$	$(TBA)_2$-$[W_6I_8I_6]$	assignments
45	60			
	84			
97	93	62	44	X−W−Y, T_{2g}
118	100	70		
	107	80		
146	117	112	82	W−W
186	162	167		W−W
195	122	128		W−X
207	129	122	94	W−X
225p	218p	161p	113p	W−Y(Y_6), A_{1g}
	167	206		
312	234	232	124	W−X
296p	197p	198p	152p	W−X(X_8), A_{1g}
262		192		W−Y
		221	174	
289p	268	271p	236p	W−W(M_6), A_{1g}
312				
338				

[a] p signifies polarized vibration where depolarization ratios were measured.

Raman band assigned to the symmetric Br_6 mode from 161 to 164 cm^{-1}. The band attributed to the A_{1g} facial W−Br stretch (Br_8 breathing motion) increases from 198 to 201 cm^{-1}. Depolarization ratio measurements could not be made on the band assigned to the symmetric W_6 cage motion in (PPN)-$[W_6Br_8Br_6]$ since the complex is soluble and stable only in CH_2Cl_2, which exhibits an intense Raman band near 280 cm^{-1}. Spectra of a powdered sample exhibit bands at 266 and 273 cm^{-1}, but on the basis of the observed lengthening of the W−W distance upon oxidation, the 273 cm^{-1} assignment is preferred.

Far-Infrared Spectra. The Raman results can be used to assist in the assignment of the bands observed in the far-infrared spectra. From the selection rules for a molecule possessing O_h symmetry, the $M_6X_8Y_6$ complexes have five T_{1u} infrared active modes. The modes consist of two M−X stretches, one M−Y stretch, one M−M stretch, and a X−M−Y bend, which is essentially a wagging motion of the Y ligand (Table 2). A lowering of symmetry due to the crystalline environment may result in more bands in the infrared spectra.

Infrared data from different studies can be combined to give reliable assignments for the molybdenum clusters.[5c,13,15] It is evident from the series $L_2[Mo_6Cl_8Y_6]$ (L = cation) that three infrared absorption bands change only slightly, suggesting association with the $Mo_6Cl_8^{4+}$ unit. One infrared band changes notably with changing Y ligand and may then be assigned to the Mo−Y mode. This band is observed near 240 cm^{-1} in the various spectra measured for $L_2[Mo_6Cl_8Cl_6]$ species and is assigned to the band at 167 cm^{-1} for $L_2[Mo_6Cl_8Br_6]$, 162 cm^{-1} for $L_2[Mo_6Br_8Br_6]$, and 132 cm^{-1} for $L_2[Mo_6Cl_8I_6]$. One Mo−X stretch is assigned to the band at 331 cm^{-1} in $(TBA)_2[Mo_6Cl_8Cl_6]$, which shifts only slightly with different Y ligands. This stretch is attributed to the 244 cm^{-1} band for $(TBA)_2[Mo_6Br_8Br_6]$. The remaining T_{1u} Mo−X mode can be assigned to the band at 220 cm^{-1} in the spectrum of $(TBA)_2[Mo_6Cl_8Cl_6]$ and to that at 148 cm^{-1} in $(TBA)_2[Mo_6Br_8Br_6]$. The infrared absorption between 350 and 360 cm^{-1} in $L_2[Mo_6Cl_8Y_6]$ complexes remains to be assigned to the Mo−Mo mode. The corresponding assignment for $(TBA)_2[Mo_6Br_8Br_6]$ is to the 324 cm^{-1} band. The X−Mo−Y bend can be assigned to the band at 108 cm^{-1} in the spectrum of $(TBA)_2[Mo_6Cl_8Cl_6]$ and to that at 75 cm^{-1} in $(TBA)_2[Mo_6Br_8Br_6]$.

The assignments of the far-infrared spectra of the tungsten clusters are in close agreement with previously published results.[14] With the complete series of $(L)_2[W_6X_8Y_6]$ and $[W_6X_8Y_4]$ complexes, the IR band assignments for the three modes associated with the $W_6X_8^{4+}$ unit and the W−Y and X−W−Y modes are straightforward. The Raman data assist in specific assignments for the modes associated with the $W_6X_8^{4+}$ unit. Accordingly, the W−W mode is attributed to the band between 250 and 270 cm^{-1} for X = Cl or Br and to that near 230 cm^{-1} for $W_6I_8^{4+}$ clusters. The two W−X vibrations can be attributed to the remaining bands associated with the $W_6X_8^{4+}$ unit.

Table 7. Comparison of Raman Shifts for the Bands Assigned to the Symmetric Modes for $(TBA)_2[W_6Br_8Br_6]$ and $(PPN)[W_6Br_8Br_6]$[a]

	$(TBA)_2[W_6Br_8Br_6]$		$(PPN)[W_6Br_8Br_6]$		
bond	ν (cm^{-1})	D (Å)	ν(observed) (cm^{-1})	ν(calculated) (cm^{-1})	D (Å)
W−W(cis)	271	2.634	266	267	2.649
W−Br(axial)	161	2.588	163	169	2.538
W−Br(facial)	198	2.628	201	201	2.613

[a] Bond distances are from ref 26 and calculations with equations are from ref 24.

Conclusions

Our spectroscopic studies have led to convincing assignments of the three totally symmetric (A_{1g}) fundamentals in $(TBA)_2[Mo_6Br_8Br_6]$, $(TBA)_2[Mo_6I_8I_6]$, $(TBA)_2[W_6Cl_8Cl_6]$, $(TBA)_2[W_6Br_8Br_6]$, and $(TBA)_2[W_6I_8I_6]$. Of particular interest is the identification of the A_{1g} M−M vibration (M_6 breathing mode), which had not been unambiguously assigned in these cluster complexes. The Raman band for this mode for $(TBA)_2[Mo_6Cl_8Cl_6]$ and closely related clusters is difficult to identify because of its low intensity. However, given calculations relating force constants and bond distances, and given the fact that the weak Raman band at 336 cm^{-1} for $[Mo_6Cl_8(Cl_4(THF)_2]$ is polarized, the Mo_6 breathing mode has been assigned for $(TBA)_2[Mo_6Cl_8Cl_6]$ and related complexes. By utilizing derivatives that possess methoxide and benzenethiolate ligands, these assignments have been verified and proposed assignments for the remaining bands forwarded. The Raman data also assist in the characterization of the far-infrared spectra of some of the molybdenum and tungsten clusters. The Raman spectra of the tungsten complexes together with the extensive infrared work of Hogue and McCarley allow for a complete picture of the vibrational spectra of the tungsten−halide clusters (Tables 6−8).[14]

In comparing the Raman spectra of the Mo and W cluster complexes, the Raman shifts for the A_{1g} M−X (X_8 face-bridging cube breathing motion) and M−Y (Y_6 cage breathing motion) band energies are shown to be surprisingly independent of the metal. The Raman band energies for the X_8 mode in the molybdenum chloride, bromide, and iodide cluster spectra are 236, 154, and 113 cm^{-1}, respectively; the corresponding values for the tungsten series are 225, 161, and 113 cm^{-1}. For the symmetric Y_6 mode, the Raman shifts are 314, 205, and 155 cm^{-1} for the Mo clusters and 296, 198, and 152 cm^{-1} for the tungsten series. Moreover, the ratios of the symmetric metal−halide Raman shifts [ν(Cl)/ν(Br) and ν(Br)/ν(I)] for both metals are approximately 1.5 and 1.3, which are equal to the square root of the inverse mass ratios of the halogens. This observation suggests, most remarkably, that the metal−halide force constants are nearly the same in these systems regardless of the identity of the metal or the halide.

The extensive mode mixing that was expected for these complexes is not evident in the Raman spectra. The results are a unique example of the applicability of a group-frequency

Table 8. Infrared Bands (cm^{-1}) and Proposed Assignments of $[M_6X_8Y_6]^{2-}$ Clusters

$[Mo_6Cl_8Cl_4]$	$(TBA)_2[Mo_6Cl_8Cl_6]$	$L_2[W_6Cl_8Br_6]$[a]	$L_2[W_6Cl_8I_6]$[a]	$(TBA)_2[Mo_6Br_8Br_6]$	assignments
120	108			75	X−Mo−Y, T_{1u}
249	248	167	132	162	Mo−Y, T_{1u}
222	221	232	229	148	Mo−X, T_{1u}
330	331	305	295	244	Mo−X, T_{1u}
351	365	360	357	324	Mo−Mo, T_{1u}

[a] From refs 5c and 15.

concept to systems where symmetry coordinates are expected to be strongly mixed in the normal modes. In addition to being largely independent of the metal, the metal−halide vibrations are also unaffected by substitution of the remaining ligands. For example, the Raman band assigned to the symmetric Cl_8 breathing motion was consistently observed at about the same frequency in all of the complexes with a $Mo_6Cl_8^{4+}$ unit, regardless of the identity of the Y ligand. The Raman shifts for the symmetric Cl_6 and Br_8 modes also change very little in the spectra of $(TBA)_2[W_6Br_8Cl_6]$, $(TBA)_2[W_6Br_8Br_6]$, and $(TBA)_2[W_6Cl_8Cl_6]$. Furthermore, the variations in the Raman band assigned to the A_{1g} M−M (M_6) mode in the different complexes are largely accounted for by differences in the M−M bond distances, rather than the mixing of modes.

Acknowledgment. We thank John Huffman for the crystal structure analysis of the thiolate derivative. Part of this work was performed at Los Alamos National Laboratory under the auspices of the U.S. Department of Energy. Research at Caltech was supported by grants from the National Science Foundation. Support from the Laboratory Directed Research and Development Project 95101 at Los Alamos (J.R.S.) with additional support by the National Science Foundation at the University of Texas at Austin (W.H.W.) and the Wrubel Computing Center at Indiana University are acknowledged.

Supporting Information Available: Tables of data for the crystal structure of $[Mo_6Cl_8(SPh)_6][NBu_4]_2$, including crystal and diffractometer data, fractional coordinates and thermal parameters, and a complete list of bond distances and angles (18 pages). Ordering information is given on any current masthead page. Additional information concerning this structure can be obtained from the Indiana University Molecular Structure Center by requesting structure report no. 83074.

IC960184B